NANO EXPRESS   **Open Access**

Synthesis, structure, and photovoltaic property of a nanocrystalline 2H perovskite-type novel sensitizer (CH$_3$CH$_2$NH$_3$)PbI$_3$

Jeong-Hyeok Im[1], Jaehoon Chung[2], Seung-Joo Kim[2] and Nam-Gyu Park[1*]

Abstract

A new nanocrystalline sensitizer with the chemical formula (CH$_3$CH$_2$NH$_3$)PbI$_3$ is synthesized by reacting ethylammonium iodide with lead iodide, and its crystal structure and photovoltaic property are investigated. X-ray diffraction analysis confirms orthorhombic crystal phase with $a = 8.7419(2)$ Å, $b = 8.14745(10)$ Å, and $c = 30.3096(6)$ Å, which can be described as 2 H perovskite structure. Ultraviolet photoelectron spectroscopy and UV-visible spectroscopy determine the valence band position at 5.6 eV versus vacuum and the optical bandgap of *ca.* 2.2 eV. A spin coating of the CH$_3$CH$_2$NH$_3$I and PbI$_2$ mixed solution on a TiO$_2$ film yields *ca.* 1.8-nm-diameter (CH$_3$CH$_2$NH$_3$) PbI$_3$ dots on the TiO$_2$ surface. The (CH$_3$CH$_2$NH$_3$)PbI$_3$-sensitized solar cell with iodide-based redox electrolyte demonstrates the conversion efficiency of 2.4% under AM 1.5 G one sun (100 mW/cm^2) illumination.

Keywords: (CH$_3$CH$_2$NH$_3$)PbI$_3$, 2H perovskite, Dye-sensitized solar cell, Nanodot, Sensitizer

Background

Semiconductor nanocrystals have received much attention due to quantum confinement effect, in which the continuous optical transitions between the electronic bands in the bulk crystals become discrete in the nanocrystals and thereby the properties of the nano-sized materials become size-dependent [1-3]. The size-dependent optical properties of semiconductor n anoparticles have been widely applied in displays [4], biomedical imaging sensors [5], and photovoltaic solar cells [6]. In the case of solar cell application, semiconductor nanomaterials can be used as a light-absorbing material (photosensitizer) in either a solid-state pn junction structure or a photoelectrochemical junction type [7]. Dispersion of semiconductor nanocrystal on a high-surface-area n-type or p-type support is an effective method to utilize it as a photosensitizer. For this reason, semiconductor (or quantum dot)-sensitized solar cell has recently attracted a lot of interest [8,9]. As photosensitizers in the semiconductor-sensitized solar cell, metal chalcogenides have been mostly studied, where Sb$_2$S$_3$-sensitized solar cell demonstrated a conversion efficiency as high as 6.18%

at simulated one sun (100 mW/cm^2) illumination [10]. Recently, a conversion efficiency of 6.54% at one sun was reported based on perovskite semiconductor (CH$_3$NH$_3$) PbI$_3$ [11], where (CH$_3$NH$_3$)PbI$_3$ was found to form *in situ* on a nanocrystalline TiO$_2$ surface from spin coating of the CH$_3$NH$_3$I and PbI$_2$ mixed solution. Moreover, an organic–inorganic hybrid perovskite structure has advantage over other crystal structures as for the sensitizer since it has high light absorption property and thermal stability as well. Since the perovskite ABX$_3$ structure was known to be stabilized depending on the ionic radii of A and B cations in relation with tolerance factor [12,13], it can be possible to tailor a new perovskite-type semiconductor sensitizer by substituting methylammonium cation in the cuboctahedral A site with longer alkyl-chain ammonium cations. Change in the A-site cation is expected to tune the bandgap energy of alkylammonium lead iodide perovskite sensitizer due to change in chemical boding nature. Here, we report for the first time on the synthesis and structural analysis of (CH$_3$CH$_2$NH$_3$)PbI$_3$. Valence band position and optical bandgap are evaluated by ultraviolet photoelectron spectroscopy (UPS) and UV-visible (UV–vis) spectroscopy, respectively. Photovoltaic performance of a (CH$_3$CH$_2$NH$_3$) PbI$_3$-sensitized solar cell is investigated in the presence of an iodide-based redox electrolyte.

* Correspondence: npark@skku.edu
[1]School of Chemical Engineering and Department of Energy Science, Sungkyunkwan University, Suwon 440-746, Republic of Korea
Full list of author information is available at the end of the article
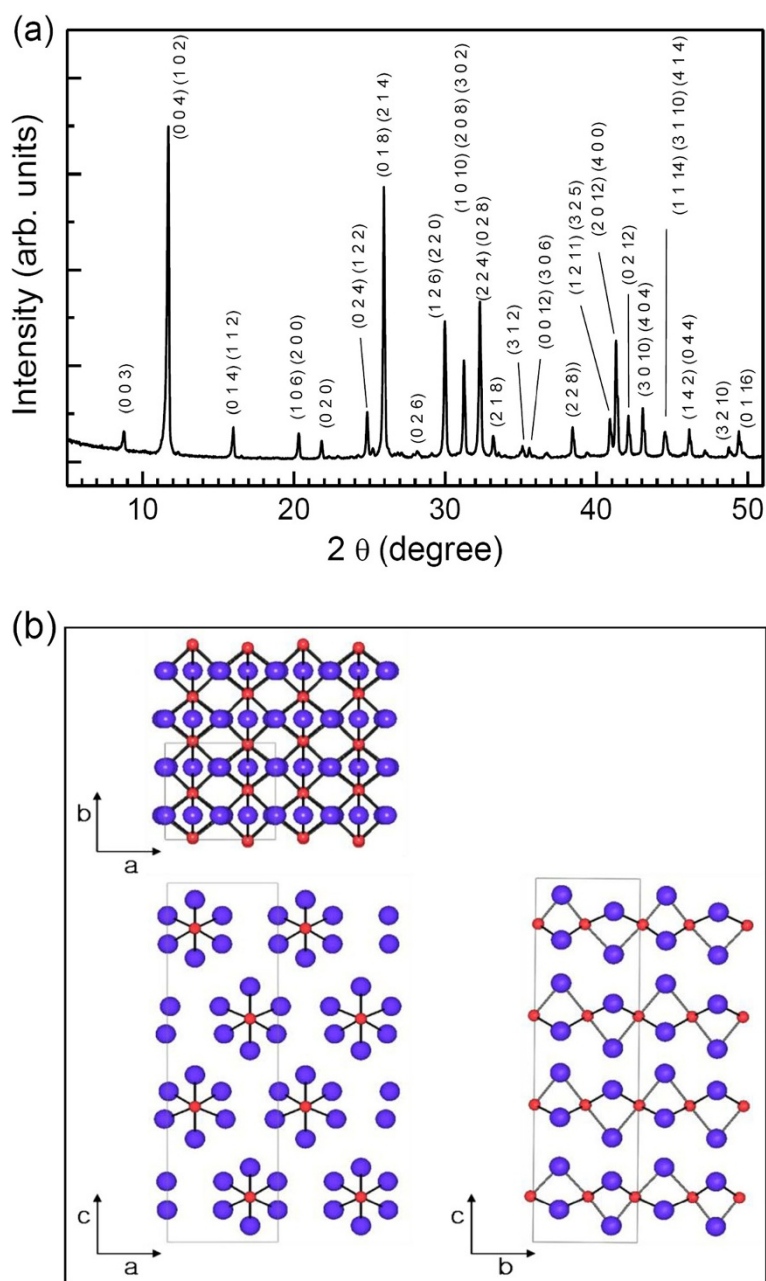
Figure 1 Powder XRD pattern (a) and crystal structure (b) of (CH$_3$CH$_2$NH$_3$)PbI$_3$. Red and purple spheres represent Pb and I ions, respectively.

Methods

The semiconductor sensitizer of (CH$_3$CH$_2$NH$_3$)PbI$_3$ was prepared by direct deposition of the γ-butyrolactone (Aldrich, Sigma-Aldrich Corporation, St. Louis, MO, USA) solution with equimolar CH$_3$CH$_2$NH$_3$I and PbI$_2$ on a nanocrystalline TiO$_2$ surface. CH$_3$CH$_2$NH$_3$I was synthesized by reacting 18.2 mL of ethylamine (2.0 M in methanol, Aldrich) and 10 mL of hydroiodic acid (57 wt.% in water, Aldrich) in a 250-mL round-bottomed flask at 0°C for 2 h. The precipitate was collected by evaporation at 80°C for

1 h, which is followed by washing three times with diethyl ether and then finally dried at 100°C in a vacuum oven for 24 h. The synthesized CH$_3$CH$_2$NH$_3$I powder was mixed with PbI$_2$ (Aldrich) at a 1:1 mole ratio in γ-butyrolactone at 80°C for 2 h, which was used as a coating solution for the *in situ* formation of (CH$_3$CH$_2$NH$_3$)PbI$_3$ on the TiO$_2$ surface. The concentration of the coating solution was 42.17 wt.%, which contains 2.234 g of CH$_3$CH$_2$NH$_3$I (12.9 mmol) and 6.016 g of PbI$_2$ (12.9 mmol) in 10 mL of γ-butyrolactone.

Table 1 Miller indices (*hkl*), spacing of lattice plane (*d*), and XRD peak intensity (*I*) of (CH$_3$CH$_2$NH$_3$)PbI$_3$

hkl	d_{obs}	d_{cal}	I_{obs}
(0 0 3)	10.06	10.08	9
(0 0 4) (1 0 2)	7.552	7.552	100
(0 1 4) (1 1 2)	5.532	5.530	11
(1 0 6) (2 0 0)	4.357	4.360	9
(0 2 0)	4.057	4.060	6
(0 2 4) (1 2 2)	3.574	3.576	15
(0 1 8) (2 1 4)	3.422	3.424	82
(0 2 6)	3.158	3.161	3
(1 2 6) (2 2 0)	2.97	2.972	43
(1 0 10) (2 0 8) (3 0 2)	2.852	2.855	30
(0 2 8) (2 2 4)	2.763	2.765	48
(2 1 8)	2.691	2.693	8
(3 1 2)	2.548	2.693	4
(0 0 12) (3 0 6)	2.516	2.518	4
(2 2 8)	2.334	2.335	10
(1 2 11) (3 2 5)	2.199	2.201	12
(2 0 12) (4 0 0)	2.179	2.180	34
(0 2 12)	2.139	2.140	13
(3 0 10) (4 0 4)	2.093	2.095	15
(1 1 14) (3 1 10) (4 1 4)	2.028	2.028	9
(0 4 4) (1 4 2)	1.961	1.961	10
(3 2 10)	1.863	1.862	5
(0 1 16)	1.838	1.846	9

Table 2 Unit cell, positional, and thermal parameters for (CH$_3$CH$_2$NH$_3$)PbI$_3$

Space group: Pmmn

a = 8.7419(2) Å, *b* = 8.14745(10) Å, *c* = 30.3096(6) Å, *Z* = 8

R_p = 15.3% R_{wp} = 21.0% R_{exp} = 9.47% χ^2 = 4.9

|	Site	*x*	*y*	*z*	B(Å^2)[a]
Pb1	4*e*	0.75	0.5261(17)	0.1256(12)	0.66(15)
Pb2	4*e*	0.25	0.493(2)	0.3776(10)	0.66(15)
I1	2*a*	0.25	0.25	0.466(2)	3.4(2)
I2	2*a*	0.75	0.75	0.046(2)	3.4(2)
I3	2*b*	0.75	0.25	0.208(2)	3.4(2)
I4	2*b*	0.25	0.75	0.288(2)	3.4(2)
I5	4*f*	0.997(6)	0.25	0.0898(13)	3.4(2)
I6	4*f*	0.993(6)	0.75	0.1693(13)	3.4(2)
I7	4*f*	0.526(6)	0.25	0.3429(12)	3.4(2)
I8	4*f*	0.013(6)	0.75	0.4195(14)	3.4(2)

Structural parameters for C, N, and H atoms were not refined. [a]All of the isotropic atomic displacement parameters (*B*) of each atomic species were constrained to have the same values.
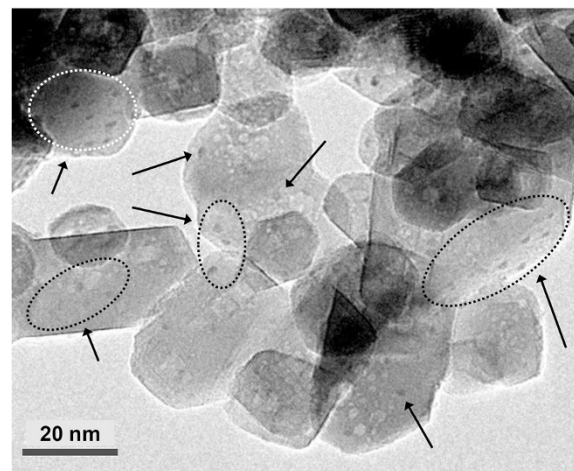
Figure 2 TEM image of the (CH$_3$CH$_2$NH$_3$)PbI$_3$–deposited TiO$_2$ nanoparticles. Arrows indicate (CH$_3$CH$_2$NH$_3$)PbI$_3$ nanodots.

Nanocrystalline TiO$_2$ particles were prepared by hydrothermal method at 230°C, and non-aqueous TiO$_2$ paste was prepared according to the method reported elsewhere [14]. Fluorine-doped tin oxide (FTO) conductive glass (TEC-8, 8 Ω/sq, Pilkington, St Helens, UK) was pretreated with 0.1 M Ti(IV) bis(ethyl acetoacetato)-diisopropoxide (Aldrich) in 1-butanol (Aldrich) solution, in which the nanocrystalline TiO$_2$ paste was deposited and heated at 550°C for 1 h. The thicknesses of the annealed TiO$_2$ films were determined by an alpha-step IQ surface profiler (KLA-Tencor Corporation, Milpitas, CA, USA). The perovskite coating solution was spread on the annealed TiO$_2$ film (38.46 μL/cm^2) and was spun for 10 s at a speed of 2,000 rpm in ambient atmosphere. The perovskite (CH$_3$CH$_2$NH$_3$)PbI$_3$ formed on the TiO$_2$ surface was dried at 100°C for 15 min. Pt counter electrode was prepared by spreading a droplet of 7 mM H$_2$PtCl$_6$*x*H$_2$O in 2-propanol on a FTO substrate and heated at 400°C for 20 min in air. The (CH$_3$CH$_2$NH$_3$)PbI$_3$-sensitized TiO$_2$ working electrode and the counter electrode were sandwiched using 25-μm-thick Surlyn (SX1170-25, Solaronix SA, Aubonne, Switzerland). The redox electrolyte was prepared by dissolving 0.9 M LiI (Aldrich), 0.45 M I$_2$ (Aldrich), 0.5 M *tert*-butylpyridine(Aldrich), and 0.05 M urea (Aldrich) in ethyl acetate (Aldrich), which was introduced into the space of the sealed electrodes prior to measurement.

Powder X-ray diffraction (XRD) profiles were recorded on a Rigaku D/MAX-2200/PC diffractometer (Tokyo, Japan) using graphite-monochromated CuKα radiation (λ = 1.5418 Å). Data were collected over the 2θ range from 5° to 100° for 4 s in each 0.02° step at ambient temperature. The TREOR software [15] was used for indexing and determining the lattice parameters. For XRD measurement,
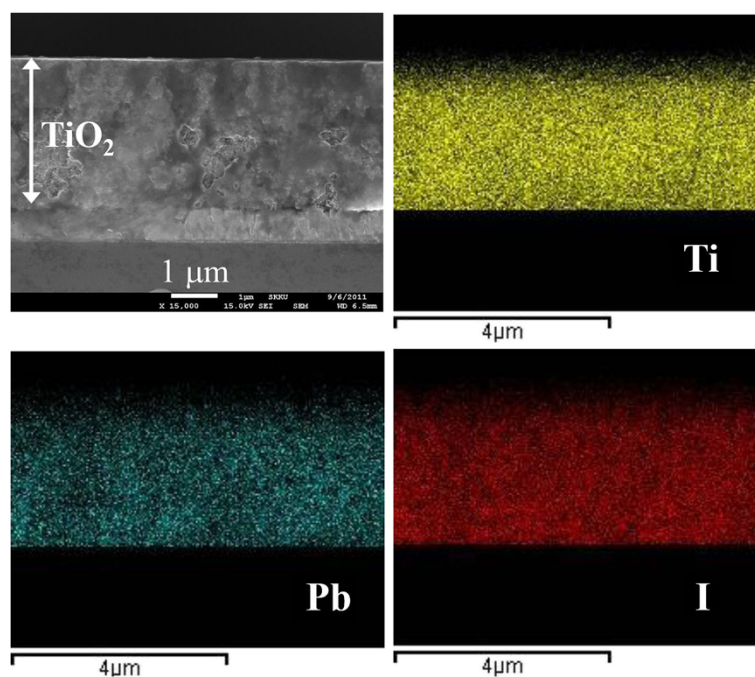
Figure 3 Cross-sectional SEM micrographs of $(CH_3CH_2NH_3)PbI_3$-deposited TiO_2 film and EDS maps for titanium, lead, and iodine.

$(CH_3CH_2NH_3)PbI_3$ powder was obtained by drying the solution of the equimolar mixture of $CH_3CH_2NH_3I$ and PbI_2 at 100°C. Photocurrent and voltage were measured from a solar simulator equipped with a 450-W xenon lamp (6279NS, Newport Corporation, Irvine, CA, USA) and a Keithley 2400 source meter (Cleveland, OH, USA). Light intensity was adjusted with the NREL-calibrated Si solar cell having KG-2 filter for approximating one-sun light intensity (100 mW/cm^2). While measuring current and voltage, the cell was covered with a black mask having an aperture, where the aperture area was slightly smaller than the active area. Distribution of perovskite $(CH_3CH_2NH_3)$ PbI_3 in the TiO_2 film was investigated by a distribution mapping technique using an energy-dispersive X-ray spectroscope (EDS) combined with a field-emission scanning electron microscope (FE-SEM, Jeol JSM 6700 F). X-ray energies corresponding to Ti, Pb, and I were collected as the SEM scanned the electron beam over the surface and cross-sectional area in the TiO_2 film. The X-ray data were synchronized with the SEM image, and an elemental mapping was created showing the presence of the selected element throughout the selected area. Transmission electron microscope (TEM) image was investigated using high-resolution TEM (HR-TEM, Jeol, JEM-2100 F) at an acceleration voltage of 200 kV. The UV–vis reflectance spectra of the powdered $(CH_3CH_2NH_3)PbI_3$, the $(CH_3CH_2NH_3)PbI_3$-adsorbed TiO_2 nanoparticle, and the bare TiO_2 particle were recorded using a UV/VIS/NIR spectrophotometer (Lambda 950 model, PerkinElmer, Waltham, MA, USA) in

a wavelength of 200 to 1,100 nm. UPS equipped with He-I source (hv = 21.22 eV) (AXIS Nova, Kratos Analytical Ltd., Manchester, UK) was used to determine the valence band energy of $(CH_3CH_2NH_3)PbI_3$.

Results and discussion

Figure 1a shows the XRD pattern of the synthesized $(CH_3CH_2NH_3)PbI_3$. All reflections are indexed by an orthorhombic unit cell with $a = 8.7419(2)$ Å, $b = 8.14745$ (10) Å, $c = 30.3096(6)$ Å. Reflection conditions ($h + k = 2n$ for $hk0$, $h = 2n$ for $h00$, and $k = 2n$ for $0k0$) observed in the XRD pattern indicate that possible space groups are $P2_1mn$ and $Pmmn$ (Table 1). By assuming a centrosymmetric space group $Pmmn$, the structural parameters for heavy atoms such as Pb and I are determined by applying the direct method using the EXPO software [16] and refined by the Rietveld method with the FULLPROF program [17]. Table 2 shows the atomic coordinates, isotropic temperature factors, and agreement factors. The structural information about C, N, and H atoms could not be obtained due to the low resolution of the laboratory XRD equipment. As shown in Figure 1b, the structure of $(CH_3CH_2NH_3)PbI_3$ can be described as a 2 H perovskite type which consists of infinite chains of face-sharing (PbI_6) octahedra running along the b-axis of the unit cell. These chains are separated from one another by ethylammonium ions.

Figure 2 shows TEM image of the $(CH_3CH_2NH_3)PbI_3$ deposited on TiO_2 nanoparticles, where the $(CH_3CH_2NH_3)$
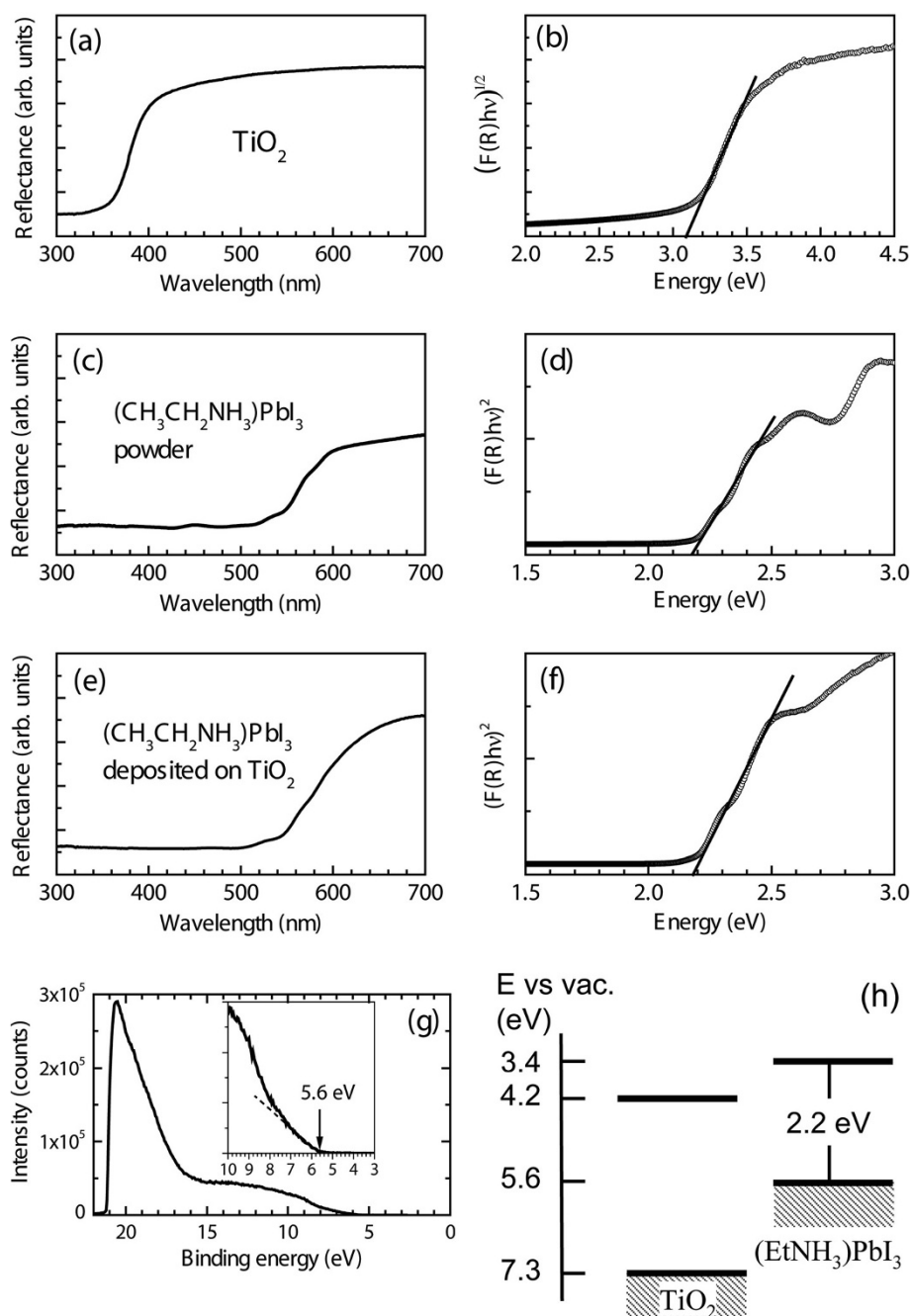
Figure 4 Diffuse reflectance spectra, UPS spectrum, and schematic energy profile for (CH₃CH₂NH₃)PbI₃. Diffuse reflectance spectra and the transformed Kubelka-Munk function for (**a**, **b**) the bare TiO_2, (**c**, **d**) the powdered $(CH_3CH_2NH_3)PbI_3$, and (**e**, **f**) the $(CH_3CH_2NH_3)PbI_3$ deposited on TiO_2. (**g**) UPS spectrum and (**h**) schematic energy profile for $(CH_3CH_2NH_3)PbI_3$. In UPS spectrum, binding energy was adjusted with respect to He-I (21.22 eV).

PbI_3 dots are clearly seen and sparsely distributed on the TiO_2 surface. This indicates that spin coating of the solution containing $CH_3CH_2NH_3I$ and PbI_2 leads to $(CH_3CH_2NH_3)PbI_3$ dots on the TiO_2 surface. The average size of the deposited $(CH_3CH_2NH_3)PbI_3$ is estimated to be about 1.8 nm in diameter.

Figure 3 shows cross-sectional EDS mapping, where Pb and I are well distributed three-dimensionally in the mesoporous TiO_2 film. Atomic percentages from EDS elemental analysis are found to be 1.66% and 4.74% for Pb and I, respectively, which indicates that the ratio of Pb to I is close to 1:3.
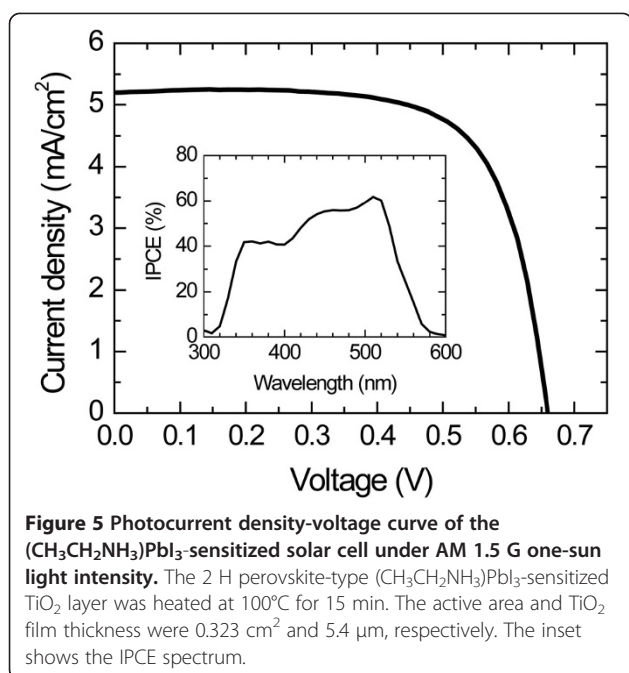
Figure 5 Photocurrent density-voltage curve of the (CH$_3$CH$_2$NH$_3$)PbI$_3$-sensitized solar cell under AM 1.5 G one-sun light intensity. The 2 H perovskite-type (CH$_3$CH$_2$NH$_3$)PbI$_3$-sensitized TiO$_2$ layer was heated at 100°C for 15 min. The active area and TiO$_2$ film thickness were 0.323 cm^2 and 5.4 μm, respectively. The inset shows the IPCE spectrum.

To determine optical bandgap and valence band position, UV–vis reflectance and UPS measurements are performed. Figure 4a,b,c,d,e,f shows the diffuse reflectance spectra and the transformed Kubelka-Munk spectra for the bare TiO$_2$ nanoparticle, the powdered (CH$_3$CH$_2$NH$_3$)PbI$_3$, and the deposited (CH$_3$CH$_2$NH$_3$)PbI$_3$ on the TiO$_2$ surface. The dependence of the optical absorption coefficient with the photon energy has been known to help to study the type of transition of electrons and semiconductors' bandgap energy as well [18]. The optical absorption coefficient (α) can be calculated using reflectance data according to the Kubelka-Munk equation [19], $F(R) = \alpha = \frac{(1-R)^2}{2R}$, where R is the reflectance data. The incident photon energy (hv) and the optical bandgap energy (E_g) are related to the transformed Kubelka-Munk function, $[F(R)\mathrm{hv}]^{\frac{1}{p}} = A(\mathrm{hv} - E_g)$, where A is the constant depending on transition probability and p is the index that is related to the optical absorption process. Theoretically, p equals to 2 or ½ for an indirect or direct allowed transition, respectively. The E_g of the bare TiO$_2$ determined based on indirect transition is 3.1 eV, which is well consistent with the data reported elsewhere [19]. For the case of (CH$_3$CH$_2$NH$_3$)PbI$_3$, a transformed Kubelka-Munk function can be constructed by plotting $[F(R)]^2$ against the photon energy, which is indicative of direct transition. As shown in Figure 4c,d,e,f, an E_g of *ca.* 2.2 eV is estimated for both the powdered (CH$_3$CH$_2$NH$_3$)PbI$_3$ and the deposited one. According to UPS spectrum, the valence band energy (E_{VB}) of (CH$_3$CH$_2$NH$_3$)PbI$_3$ is determined to be 5.6 eV with respect to vacuum level. Therefore, from the E_g and the E_{VB} values, conduction band energy (E_{CB}) is

estimated to be 3.4 eV, which is 0.8 eV higher than that of the E_{CB} for TiO$_2$ (4.2 eV versus vacuum).

Figure 5 shows the photovoltaic property of the (CH$_3$CH$_2$NH$_3$)PbI$_3$-sensitized solar cell, where I$_3^-$/I$^-$ redox electrolyte is employed. A photocurrent density of 5.2 mA/cm^2, a voltage of 0.660 V, and a fill factor of 0.704 are observed at AM 1.5 G one sun (100 mW/cm^2) illumination, leading to an overall conversion efficiency of 2.4%. Incident photon-to-current conversion efficiency (IPCE) spectrum shows that the electron excitation starts to occur at around 570 nm, which is consistent with the estimated E_g of *ca.* 2.2 eV.

Conclusions

We synthesized a new nanocrystalline sensitizer based on organic–inorganic hybridization. The crystal structure of the synthesized (CH$_3$CH$_2$NH$_3$)PbI$_3$ was determined to be 2 H perovskite-type orthorhombic phase. The optical bandgap was estimated to be *ca.* 2.2 eV, and the valence band energy position was determined to be 5.6 eV based on UPS measurement. The conduction band edge position of (CH$_3$CH$_2$NH$_3$)PbI$_3$ was 0.8 eV higher than that of TiO$_2$, which allowed injection of photo-excited electrons from (CH$_3$CH$_2$NH$_3$)PbI$_3$ to TiO$_2$. Under full sun illumination, the (CH$_3$CH$_2$NH$_3$)PbI$_3$-sensitized solar cell showed an overall conversion efficiency of 2.4%.

Authors' contributions
J-HI carried out the synthesis of perovskite materials and the fabrication of solar cell devices. JC and S-JK carried out the X-ray diffraction measurement and structure analysis. N-GP contributed to the conception and design of experiments, data interpretation, and writing of the manuscript. All authors read and approved the final manuscript.

Author details
[1]School of Chemical Engineering and Department of Energy Science, Sungkyunkwan University, Suwon 440-746, Republic of Korea. [2]Department of Chemistry, Division of Energy Systems Research, Ajou University, Suwon 443-749, Republic of Korea.

References
1. Alivisatos AP: **Perspectives on the physical chemistry of semiconductor nanocrystals.** *J Phys Chem* 1996, **100:**13226.
2. Alivisatos AP: **Semiconductor clusters, nanocrystals, and quantum dots.** *Science* 1996, **271:**933.
3. Gaponenko: *Optical properties of semiconductor nanocrystals.* Cambridge: Cambridge University Press; 1998.

4. Lee J, Sundar VC, Heine JR, Bawendi MG, Jensen KF: **Full color emission from II-VI semiconductor quantum dot-polymer composites.** *Adv Mater* 2000, **12:**1311.
5. Michalet X, Pinaud FF, Bentolila LA, Tsay JM, Doose S, Li JJ, Sundaresan G, Wu AM, Gambhir SS: **Quantum dots for live cells, in vivo imaging, and diagnostics.** *Science* 2005, **307:**538.
6. Nozik AJ: **Quantum dot solar cells.** *Physica E* 2002, **14:**115.
7. Hetsch F, Xu XQ, Wang HK, Kershaw SV, Rogach AL: **Semiconductor nanocrystal quantum dots as solar cell components and photosensitizers: material, charge transfer, and separation aspects of some device topologies.** *J Phys Chem Lett* 2011, **2:**1879.
8. Kamat PV: **Quantum dot solar cells. Semiconductor nanocrystals as light harvesters.** *J Phys Chem C* 2008, **112:**18737.
9. Ruhle S, Shalom M, Zaban A: **Quantum-dot-sensitized solar cells.** *Chemphyschem* 2010, **11:**2290.
10. Im SH, Lim CS, Chang JA, Lee YH, Maiti N, Kim HJ, Nazeeruddin MdK, Grätzel M, Seok SI: **Toward interaction of sensitizer and functional moieties in hole-transporting materials for efficient semiconductor-sensitized solar cells.** *Nano Lett* 2011, **11:**4789.
11. Im JH, Lee CR, Lee JW, Park SW, Park NG: **6.5% efficient perovskite quantum-dot-sensitized solar cell.** *Nanoscale* 2011, **3:**4088.
12. Pena MA, Fierro JLG: **Chemical structures and performance of perovskite oxides.** *Chem Rev* 1981, **2001:**101.
13. Bhalla AS, Guo RY, Roy R: **The perovskite structure–a review of its role in ceramic science and technology.** *Mater Res Innov* 2000, **4:**3.
14. Kim MJ, Lee CR, Jeong WS, Im JH, Ryu TI, Park NG: **Unusual enhancement of photocurrent by incorporation of Bronsted base thiourea into electrolyte of dye-sensitized solar cell.** *J Phys Chem C* 2010, **114:**19849.
15. Werner PE, Eriksson L, Westdahl M: **TREOR, a semi-exhaustive trial-and-error powder indexing program for all symmetries.** *J Appl Cryst* 1985, **18:**367.
16. Altamore A, Cascarano G, Giacovazzo C, Guagliardi A, Burla MC, Polidori G, Camalli M: ***SIR*92–a program for automatic solution of crystal structures by direct methods.** *J Appl Cryst* 1994, **27:**435.
17. Rodriguez-Carvajal J: *FULLPROF 2000: A Rietveld Refinement and Pattern Matching Analysis Program*. France: Laboratoire Léon Brillouin (CEA-CNRS); 2008.
18. Tauc J, Grigorovici R, Vancu A: **Optical properties and electronic structure of amorphous germanium.** *Phys Stat Sol (b)* 1966, **15:**627.
19. Lin H, Huang CP, Li W, Ni C, Shah SI, Tseng YH: **Size dependency of nanocrystalline TiO_2 on its optical property and photocatalytic reactivity exemplified by 2-chlorophenol.** *Appl Catal B-Environ* 2006, **68:**1.